JACS
JOURNAL OF THE AMERICAN CHEMICAL SOCIETY

Article

pubs.acs.org/JACS

Biocompatible Polymeric Nanoparticles Degrade and Release Cargo in Response to Biologically Relevant Levels of Hydrogen Peroxide

Caroline de Gracia Lux, Shivanjali Joshi-Barr, Trung Nguyen, Enas Mahmoud, Eric Schopf, Nadezda Fomina, and Adah Almutairi*

Skaggs School of Pharmacy and Pharmaceutical Sciences, Departments of NanoEngineering and of Materials Science and Engineering, University of California at San Diego, La Jolla, California 92093, United States

Supporting Information

ABSTRACT: Oxidative stress is caused predominantly by accumulation of hydrogen peroxide and distinguishes inflamed tissue from healthy tissue. Hydrogen peroxide could potentially be useful as a stimulus for targeted drug delivery to diseased tissue. However, current polymeric systems are not sensitive to biologically relevant concentrations of H_2O_2 (50−100 μM). Here we report a new biocompatible polymeric capsule capable of undergoing backbone degradation and thus release upon exposure to such concentrations of hydrogen peroxide. Two polymeric structures were developed differing with respect to the linkage between the boronic ester group and the polymeric backbone: either direct (**1**) or via an ether linkage (**2**). Both polymers are stable in aqueous solution at normal pH, and exposure to peroxide induces the removal of the boronic ester protecting groups at physiological pH and temperature, revealing phenols along the backbone, which undergo quinone methide rearrangement to lead to polymer degradation. Considerably faster backbone degradation was observed for polymer **2** over polymer **1** by NMR and GPC. Nanoparticles were formulated from these novel materials to analyze their oxidation triggered release properties. While nanoparticles formulated from polymer **1** only released 50% of the reporter dye after exposure to 1 mM H_2O_2 for 26 h, nanoparticles formulated from polymer **2** did so within 10 h and were able to release their cargo selectively in biologically relevant concentrations of H_2O_2. Nanoparticles formulated from polymer **2** showed a 2-fold enhancement of release upon incubation with activated neutrophils, while controls showed a nonspecific response to ROS producing cells. These polymers represent a novel, biologically relevant, and biocompatible approach to biodegradable H_2O_2-triggered release systems that can degrade into small molecules, release their cargo, and should be easily cleared by the body.

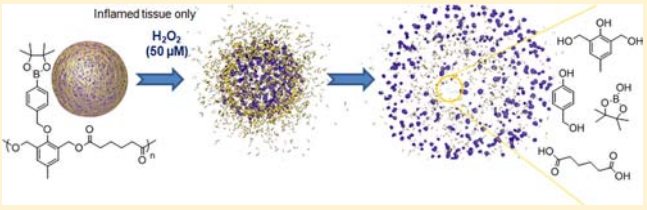

INTRODUCTION

The contribution of oxidative stress and reactive oxygen species (ROS) to the development of numerous diseases has resulted in a research focus to create ROS-specific detection systems[1−7] and ROS-responsive micro-[7] or nanocarriers.[8−13] Oxidative stress is a condition in which the balance of oxidative and reducing species within cellular environments has been disturbed. Once out of balance, ROS such as superoxide, hydrogen peroxide, and hydroxide radicals can damage cellular components.[14] Although some ROS are key to cell signaling[15] and defense mechanisms, these chemicals also contribute to various diseases.[16−18]

Methods of selective delivery of therapeutic and diagnostic reagents to sites undergoing oxidative stress would prove useful for the numerous diseases characterized by high concentrations of ROS. Polymer-based nano- and microparticles are especially useful because they can be tailored to degrade upon encountering certain stimuli,[19] such as enzymatic removal of a protecting group,[20,21] pH,[22−24] light,[25,26] and H_2O_2.[3,5,10,27,28] Upon encapsulation, nanoparticles can provide improved pharmacokinetics, as the therapeutic drug is protected from the physiological environment and selected release allows for lower drug loading through effective site delivery.[29] To our knowledge, there are few if any polymeric systems able to undergo degradation and cargo release on encountering biologically relevant (50−100 μM) H_2O_2 concentrations. One important study showed a polymeric carrier responsive to 1 mM H_2O_2 in a useful time frame using dextran reversibly modified with aryl boronic esters; this system utilized a carbonate ester linkage and took advantage of a solubility switching mechanism to release its payload.[8] Notably, this study also demonstrated the advantage of such boronic ester stabilized nanomaterials for promoting immune activation by antigen-presenting cells.

In this paper, we report a complementary polymeric system specifically sensitive to biologically relevant concentrations of H_2O_2, where aryl boronic ester protecting groups are introduced into each motif of our polymeric nanoparticle design.[26] This results in an amplification of the H_2O_2 sensitivity, because each cleavage of the boronic ester leads to polymer backbone degradation. High molecular weight polymers can be formulated into particles, and such degradation of the polymer backbone is likely responsible for

Received: April 8, 2012
Published: September 4, 2012

   dx.doi.org/10.1021/ja303372u | J. Am. Chem. Soc. 2012, 134, 15758−15764

this system's high sensitivity to H_2O_2. Furthermore, the degradation products are smaller molecular weight species that are predicted to be more easily cleared by the body than larger polymer molecules. Moreover, we can modulate the kinetics of degradation using two linkage strategies between the peroxide activated triggering group and the backbone. A recent study has shown that an ether linkage strategy provides both high hydrolytic stability and cleavage kinetics, though it has been only sparsely utilized.[30] This chemistry has been used most notably for the synthesis of ROS sensitive prodrugs to inhibit matrix metalloproteinase, an enzyme which is secreted as a ROS sensitive zymogen and implicated in the reperfusion injury associated with stroke.[31]

Here, we use these polymers to encapsulate small hydrophobic molecules and measure their release upon exposure to biologically relevant oxidative conditions. This new material represents an addition to the very small toolbox of systems with the potential to target drug delivery to oxidative conditions.

RESULT AND DISCUSSION

Design of H_2O_2-Sensitive Polymers. Polymers **1** and **2** (shown in Figure 1) differ in the linkage type between the

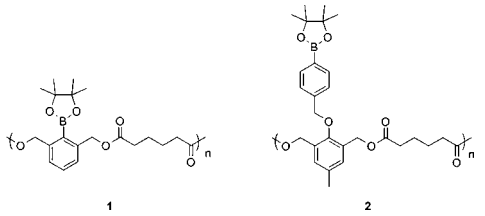

Figure 1. Chemical structures of polymers **1** and **2**.

pendant boronic ester protecting groups and the polymer backbone. Polymer **1** has a direct linkage between the polymer backbone and the protecting group, while polymer **2** has a benzylic ether boronic ester pendant to the backbone.

Mechanism of H_2O_2-Induced Polymer Degradation. Upon exposure to H_2O_2[32−34] the aryl boronic ester group is oxidized and subsequently hydrolyzed to unmask a phenol. This initiates a quinone methide rearrangement[3,31,35−37] to degrade the polymer (Scheme 1).

Monomer and Polymer Synthesis. H_2O_2 sensitive nanoparticles were formulated from polymer **1** and **2**. The synthesis of **1** (Scheme 2) began with the protection of 2,6-

Scheme 1. Mechanism of Polymeric Particle 2 Degradation upon Exposure to Hydrogen Peroxide (H_2O_2)

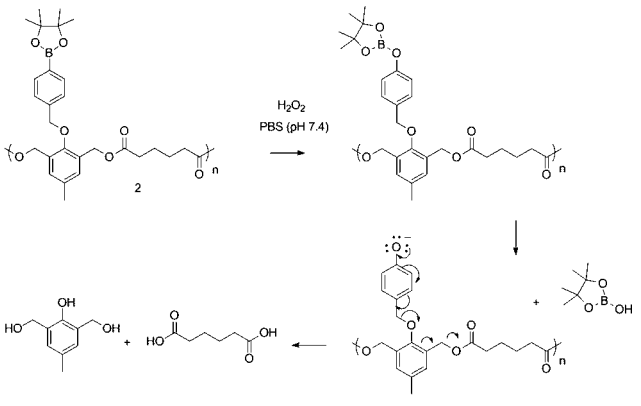

Scheme 2. Synthesis of H_2O_2 Degradable Polymers 1 and 2[a]

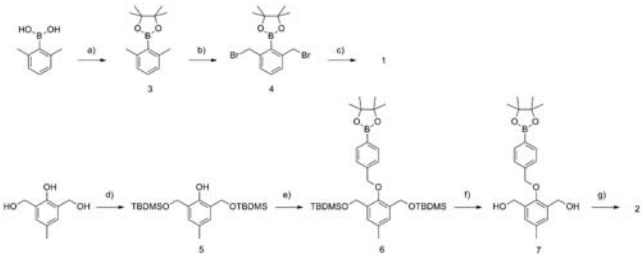

[a](a) Pinacol, C_6H_6 (84%); (b) AIBN, NBS, CCl_4 (55%); (c) adipic acid, Bu_4NOH, $CHCl_3$ (96%); (d) TBDMSCl, imidazole, DMF (95%); (e) 4-bromomethylphenyl boronic acid pinacol ester, K_2CO_3, DMF (79%); (f) *p*-TsOH, MeOH (90%); (g) adipoyl chloride, pyridine, DCM (82%).

dimethylphenylboronic acid with pinacol which afforded good yields (84%) of boronic ester **3**. Subsequent benzylic bromination with *N*-bromosuccinimide (NBS) and 2,2′-azobis-(2-methylpropionitrile) (AIBN) gave the desired monomer (55% yield). The monomer was then combined with adipic acid in the presence of a phase transfer catalyst,[38] Bu_4NOH, to give the H_2O_2 reactive polymer (PS standard: M_w = 10623, PDI = 1.9). The GPC (Figure 2, dashed line) for this polymer is not

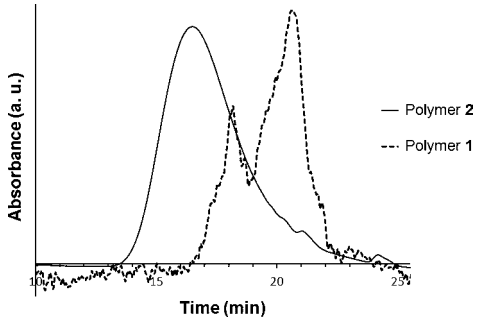

Figure 2. GPC traces of polymer **1** (M_w = 10.6 kDa, PDI = 1.9) and **2** (M_w = 51.3 kDa, PDI = 1.4).

smooth and has a high PDI, consistent with a step growth polymerization. As this direct linkage polymer is synthetically challenging,[30] we were only able to isolate short polymeric strands. However, we were able to successfully formulate particles and encapsulate Nile Red within; thus the molecular weight was sufficient for controlled release. Other methods of polymerization were extensively investigated. Pyridine in dimethyl sulfoxide (DMSO) and dimethylformamide (DMF) failed to give high conversion to polymer. 1,8-Diazabicyclo[5.4.0]undec-7-ene (DBU) in DMSO also successfully provided polymer **1** with a similar degree of polymerization. Alternative routes of polymerization were also explored, such as hydrolysis of benzyl bromide **4** followed by a subsequent reaction with adipoyl chloride. Unfortunately, the desired hydrolysis product of **4** could not be isolated.

Much better synthetic accessibility was observed for polymer **2** (Scheme 2). Polymer **2** was synthesized with slight modifications according to a previously published procedure.[26,37] First, selective protection of 2,6-bis-(hydroxymethyl)-*p*-cresol with *tert*-butyldimethylsilyl chloride (TBDMSCl) afforded **5** in good yield (95%). The phenol of **5** was then combined with 4-(hydroxymethyl)phenylboronic acid pinacol ester to provide the protected boronic ester **6**. Removal

dx.doi.org/10.1021/ja303372u | J. Am. Chem. Soc. 2012, 134, 15758−15764

of the TBS protecting groups provided monomer **7**, which is capable of copolymerization with adipoyl chloride. GPC data showed a higher degree of polymerization for **2** compared to **1** (Figure 2, solid line), which is not unexpected as the polymerization methods are different.

Nanoparticle Characterization. We formulated polymers **1** and **2** into nanoparticles via an oil/water emulsion technique. Scanning electron microscopy (SEM) and dynamic light scattering (DLS) analysis indicated the formation of nanoparticles with an average size of approximately 150 nm (Figure 3).

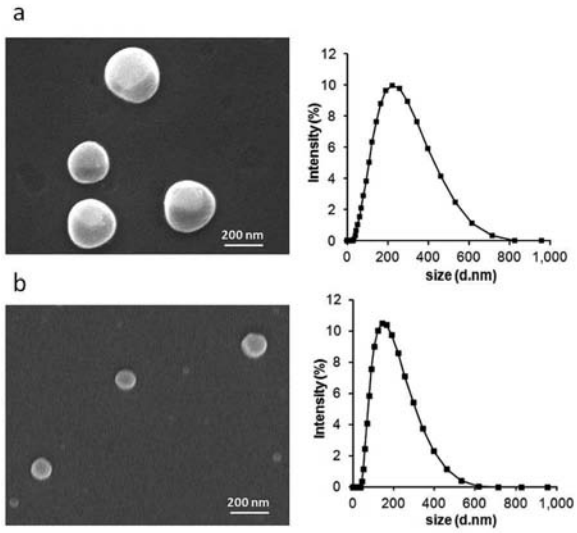

Figure 3. Characterization of polymeric particles by SEM and DLS: (a) **1** (d = 166 nm (std dev 5.7), PDI = 0.38 (std dev 0.07)) and (b) **2** (d = 136 nm (std dev 5.4), PDI = 0.30 (std dev 0.01)).

Evaluation of Controlled Release. We also formulated polymers **1** and **2** into nanoparticles encapsulating a solvatochromic dye, Nile Red, to monitor hydrogen peroxide triggered release from these polymeric nanoparticles. The encapsulation efficiency was determined by fluorescence and HPLC (50% and 44%, respectively). The fluorescence of the dye is quenched in aqueous environments, enabling use as a model compound to indicate small molecule release from the hydrophobic nanoparticle interior. Prior to the evaluation of controlled release from our materials, the stability of Nile Red fluorescence in hydrogen peroxide was tested to ensure that the fluorescence quenching observed is not a result of Nile Red exposure to hydrogen peroxide. Nile Red fluorescence does not change significantly over the course of 72 h of incubation with the highest hydrogen peroxide concentration used in our study (1 mM, Figure S1).

Exposure to 1 mM H_2O_2 (in PBS, pH = 7.4) decreased the fluorescence intensity of Nile Red in both nanoparticle formulations (Figure 4). A red shift from around 625 to 640 nm, indicating that the environment of the dye had been altered, was also observed. For nanoparticles prepared using polymer **1**, a 50% decrease in fluorescence is observed at 26 h. This result agrees with our TEM images (Figure 4b) of the degraded empty particles upon exposure to the same H_2O_2 concentration (1 mM), which indicate release of the dye. Because the nanoparticles fall apart (Figure 4), Nile Red is now exposed to a more polar medium, resulting in fluorescence quenching. In the absence of H_2O_2, Nile Red maintains 80% of its fluorescence at 622 nm over 6 days. This slight decrease may result from quenching of Nile Red adsorbed onto the surface of the particles.

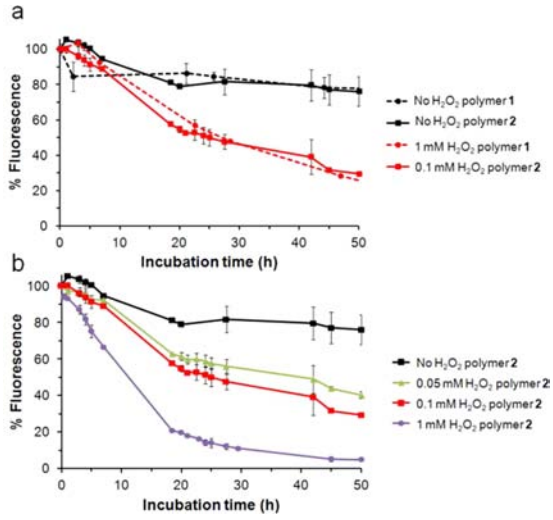

Figure 4. Fluorescence of Nile Red upon release from nanoparticles in PBS (pH 7.4) of **1** and **2** in the absence or presence of various concentrations of hydrogen peroxide, as a function of incubation time at 37 °C.

Nanoparticles made from polymer **2**, containing an ether linkage, degraded about an order of magnitude more rapidly in response to peroxide and were similarly stable in the absence of peroxide (Figure 4a). Exposure to 100 μM H_2O_2 induced a 50% decrease in Nile Red fluorescence for these nanoparticles, while those from polymer **1** required 1 mM H_2O_2 to release to the same degree. Thus, polymer **2** is sensitive to a biologically relevant concentration of H_2O_2 (50−100 μM)[39] (Figure 4b). Exposure to 1 mM H_2O_2 resulted in complete quench of the dye within a day. These release kinetics agree with the recent finding (in the context of H_2O_2 activated metalloprotein inhibitors) of faster conversion of the boronic ester to the phenol by prodrugs employing an ether linkage compared to those with a direct linkage.[30]

H_2O_2-Induced Nanoparticle Degradation. After formation and purification, nanoparticle degradation was investigated using transmission electron microscopy (TEM). Direct visualization by TEM reveals how polymer degradation affects nanoparticle structure. Contrary to indirect methods using light scattering or transmission, direct visualization of the particle morphology by TEM can detail any significant changes in the morphology of the nanoparticles after treatment with H_2O_2. Representative particles are presented; additional TEM images of particles in the absence and presence of varied concentrations of H_2O_2 (250 mM, 100 mM, 100 μM, and 50 μM) are presented in Figures S2−S6. Almost all nanoparticles are spherical and intact in the absence of H_2O_2 (Figure 5a (**1**) and 5c (**2**)). Exposure to 1 mM hydrogen peroxide induces significant ripping or crumpling of the structures, as well as particle expansion, in most particles (Figure 5b (**1**) and 5d (**2**).

Similar morphological changes were observed for nanoparticles **1** and **2** in the presence of 100 mM (3 min) or 250 mM (10 min), but the ratio between intact and degraded was much more balanced. Interestingly, for nanoparticles **2**, this combination of intact and degraded particles was also observed at low concentrations of H_2O_2 (100 and 50 μM). This supports

dx.doi.org/10.1021/ja303372u | J. Am. Chem. Soc. 2012, 134, 15758−15764

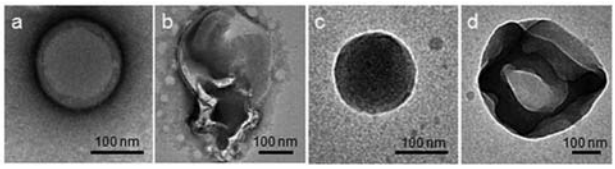

Figure 5. TEM images of nanoparticles **1** (a–b) and **2** (c–d). (a, c) After 72 h of incubation in PBS; (b, d) after 72 h in PBS containing 1 mM H_2O_2.

our conclusion that a physiological concentration of peroxide induces polymer **2** degradation.

Particle Payload Release with and without Activating ROS Production in Neutrophils. Activated neutrophils generate high levels of ROS. We measured extracellular hydrogen peroxide produced by neutrophils (differentiated mouse promyelocytes or dMPRO cells) with and without PMA (phorbol 12-myristate 13-acetate) stimulation. After 6 h of PMA treatment, 1.6×10^6 dMPRO cells produced 6.5 μM H_2O_2, while untreated cells produced 4.5 μM H_2O_2. These extracellular levels of H_2O_2 were much lower than the levels we previously used to examine polymer **2** degradation; however, the concentration of H_2O_2 inside neutrophil granules may be much higher.[40] For the release assay we chose fluorescein diacetate (FDA), a nonfluorescent molecule cleaved to fluorescein (Ex490/Em520) by cellular esterases. FDA encapsulated in nanoparticles fabricated from polymer **2**, from poly(lactic-coglycolic acid) (PLGA), and from a control polymer similar in structure to polymer **2** (with a protecting group that does not cleave in the presence of ROS[26]) were added to PMA treated and untreated dMPRO cells, and fluorescence was measured at different time points (0.5, 2, and 6 h). Release of FDA was calculated as the ratio of fluorescence from PMA treated to untreated cells (Figure 6). Overall a 2-

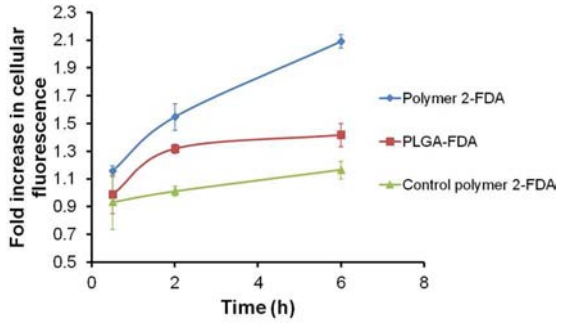

Figure 6. Fold increase in cellular fluorescence after phorbol 12-myristate 13-acetate (PMA) stimulation after 0.5, 2, and 6 h.

fold increase in release of FDA from nanoparticles of polymer **2** was observed in stimulated dMPRO cells, while PLGA showed no further release after the initial burst release observed in the first 2 h period. Nanoparticles from control polymer **2** showed a nonspecific response.

Cytotoxicity of Nanoparticles from Polymer 2. As nanoparticles from polymer **2** could provide ROS controlled cargo release upon exposure to biologically relevant oxidative conditions, we tested their cytotoxicity by Apotoxglo assay, which measures live and dead cell protease activity, to assess viability and cytotoxicity, respectively. In addition, this assay also measures caspase 3/7 activity as a readout for apoptosis (Figure 7). We compared the effect of these nanoparticles on

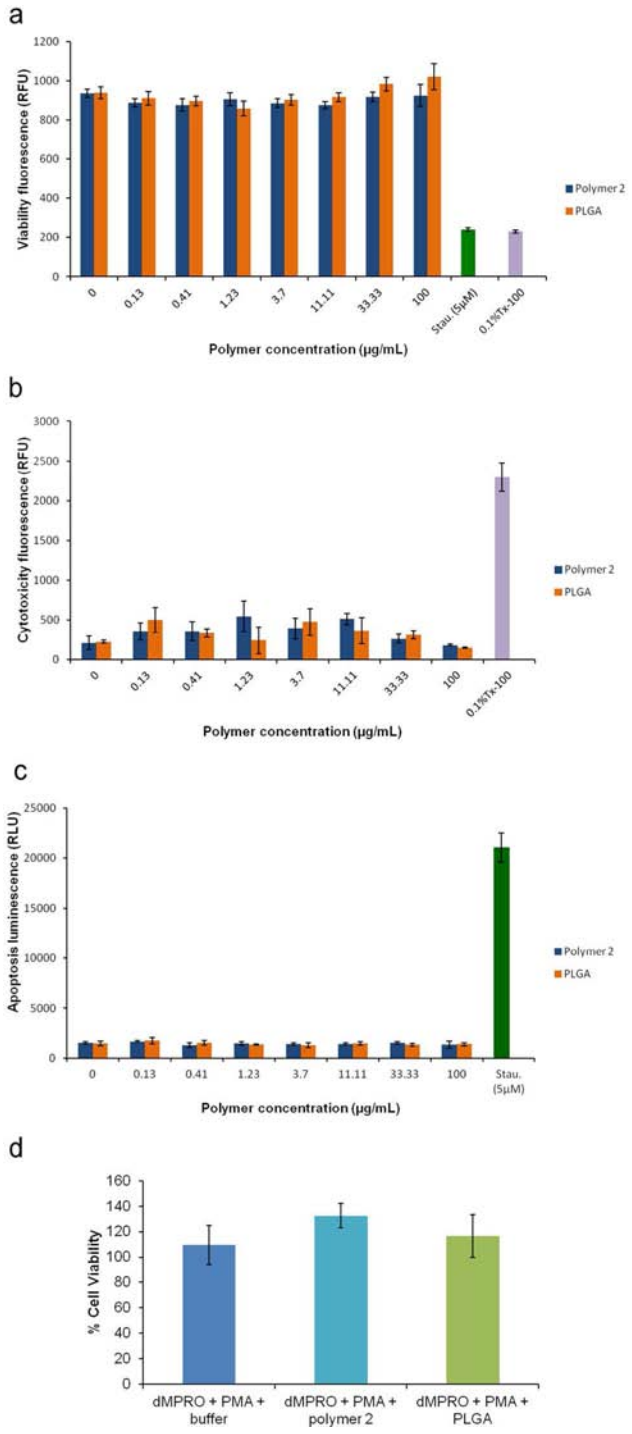

Figure 7. (a–c) Cytotoxicity analysis (a: viability, b: cytotoxicity, c: apoptosis) of the H_2O_2 degradable nanoparticles from polymer **2** and PLGA nanoparticles incubated for 5 h at different concentrations with Raw264.7 cells using Apotoxglo assay. (d) Percent cell viability of PMA-stimulated differentiated promyelocytes (dMPRO) after incubation in buffer, polymer **2** nanoparticles, and PLGA for 4 h.

Raw264.7 macrophages with that of the nontoxic FDA-approved polymer PLGA nanoparticles. Staurosporine and 0.1% Triton-X 100 were used as positive controls for induction of apoptosis and cell death, respectively. No significant differences were observed between PLGA and polymer **2** nanoparticles up to a concentration of 100 μg/mL ($p > 0.05$). Upon incubation for three different time intervals (5, 24, and

dx.doi.org/10.1021/ja303372u | J. Am. Chem. Soc. 2012, 134, 15758–15764

48h), neither polymer **2** nor PLGA induced any significant toxicity (cell death or apoptosis) compared to untreated cells (Figures 7 a–c and S7). On the other hand, apoptosis and loss of cell viability was observed in cells treated with staurospoine and 0.1% Triton X-100 (Figure 7 a–c). To test if polymer **2** nanoparticles affect the viability of activated neutrophils (which would mimic pathological conditions in vivo), we incubated polymer **2** and PLGA nanoparticles for 4 h with activated neutrophils (PMA stimulated dMPRO cells). Cell viability postincubation was measured by trypan blue staining; no loss in cell viability was seen in either case (Figure 7 d).

Polymer Degradation. After validating that degradation of polymer **2** at biologically relevant oxidative levels initiates payload release, we characterized degradation by GPC and NMR. High concentrations of H_2O_2 were used to fully degrade the polymers and confirm that the polymers degrade into predicted products (Scheme 1).

The degradation of polymer **1** was examined in 250 mM H_2O_2 in a 20% PBS/DMF (v/v) solution by gel permeation chromatography (GPC) and NMR (Figure 8). GPC following

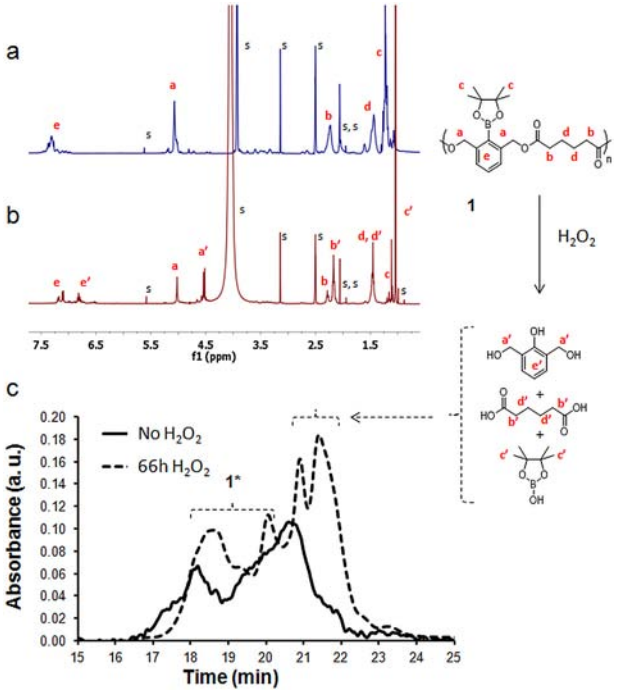

Figure 8. (a, b) ^{1}H NMR spectra of polymer **1** in DMSO-d_6, deuterium PBS (a) without H_2O_2 and (b) incubated with 500 mM H_2O_2 after 46 h at 37 °C. Solvent peaks (s) include DMSO-d_6, D_2O, and traces of water, ethyl acetate, methanol, and dichloromethane. (c) GPC chromatograms of the polymer prior to the addition of H_2O_2 (solid line) and after degradation in 20% PBS/DMF solutions containing 250 mM H_2O_2 incubated at 37 °C (dotted line). **1*** protected and deprotected polymer.

66 h of exposure to peroxide revealed small molecule peaks corresponding to products of degradation of polyester **1**, adipic acid, and 2,6-bis(hydroxymethyl)phenol (cresol) (Scheme 1) that constitute 35% of the peak area (Figure 8c). The chemical composition of the small molecule products was confirmed by NMR (Figure 8b). As the rate of polymer degradation depends on H_2O_2 concentration, high concentrations of H_2O_2 (500 mM) were used. NMR peak shifts corresponding to the formation of cresol and the liberation of adipic acid were observed; the ester bonds of the polymer degrade to carboxylic acids and alcohols. The benzyl proton peaks shift from 5.03 to 4.54 ppm, indicating a change from the ester to the benzyl alcohol. Furthermore, protons α to the ester carbonyl shifted from 2.28 to 2.16 ppm, corresponding to protons of adipic acid.

NMR shows clear evidence that the target degradation products are formed. However, chemical shifts from the remaining polymer, both protected and deprotected, are still observed by NMR (at 46 h) and by GPC (at 66 h), indicating that degradation into small molecules or oligomers is not complete in the time frame investigated. Polymer **1** thus has slow and incomplete degradation. However, this result is not unexpected, as conversion of the boronic ester to the phenol using a direct linkage strategy is slow. However, when formulated into nanoparticles, TEM and Nile Red release experiments showed that the observed polymer degradation could translate into sufficient particle degradation to result in release of an encapsulated payload.

Degradation of polymer **2** was quantified as in the case for **1**, first by ^{1}H NMR, in the absence of H_2O_2 or with 50 mM H_2O_2. As shown in Figure 9a–b, complete degradation occurred

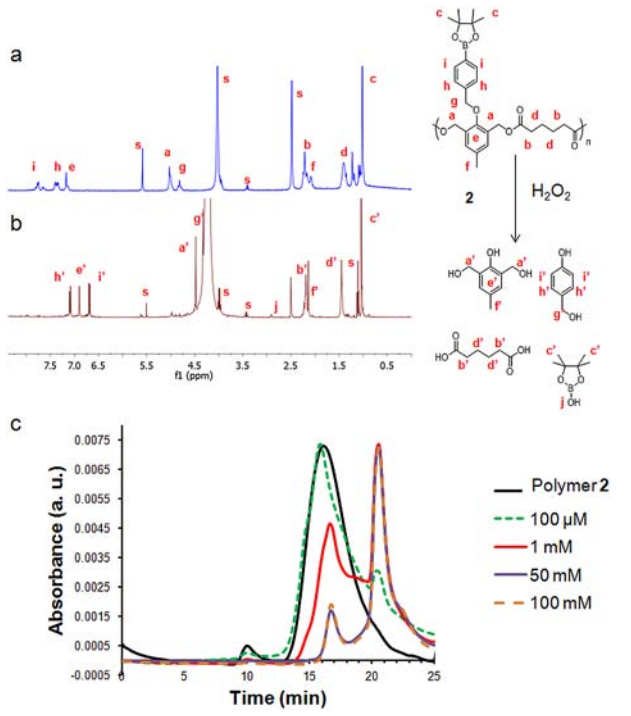

Figure 9. (a, b) ^{1}H NMR spectra of polymer **2** in DMSO-d_6, deuterium PBS (a) without H_2O_2 and (b) incubated with 50 mM H_2O_2 after 3 days at 37 °C. "s" refers to solvent peaks (DMSO-d_6, D_2O, and traces of water, ethanol, and dichloromethane). (c) GPC chromatograms of polymer **2** prior to the addition of H_2O_2 (black line) and after degradation in 20% PBS/DMF solutions containing 100 μM, 1 mM, 50 mM, and 100 mM H_2O_2 incubated at 37 °C for 1 day.

within 3 days, as broad peaks corresponding to the polymer have been replaced by the sharp peaks of the degradation products. Contrary to what has been found for **1**, H_2O_2 driven, almost complete, and fast degradation was found for **2**, and this with at least 1 order of magnitude less H_2O_2 concentration.

GPC analysis (Figure 9c) showed that polymer **2** depolymerized after only 24 h of H_2O_2 exposure at 50 mM. In agreement with the previous NMR result, the polymer

dx.doi.org/10.1021/ja303372u | J. Am. Chem. Soc. 2012, 134, 15758–15764

degraded completely after 3 days at this concentration. Interestingly, GPC reveals degradation started even with a biologically relevant H_2O_2 concentration (100 μM, green line). Importantly, neither **1** nor **2** is hydrolyzed in the absence of H_2O_2 (tested over 6 days).

CONCLUSION

In conclusion, we have synthesized a bioresponsive polyester bearing boronic ester triggering groups that degrades upon exposure to low concentrations of H_2O_2. The degradation is induced by transformation of a boronic ester to a phenol, which undergoes a quinione methide rearrangement to break down the polyester backbone. Nanoparticles formulated from the polymer degrade and release contents upon exposure to 50 μM H_2O_2. Advantages of our system are good synthetic accessibility and hydrolytic stability, fast H_2O_2 triggered cleavage kinetics, good biocompatibility, and the formation of only small degradation molecules that should be easily cleared by the body.[41]

Polymer **2** nanoparticles could be used to deliver small molecules or ROS-quenching enzymes such as catalase and superoxide dismutase to treat chronic inflammatory diseases. These diseases, such as chronic obstructive pulmonary disease (COPD) and rheumatoid arthritis, are associated with increased neutrophil recruitment.[42−45] Degranulation of neutrophils and macrophages produces ROS, which contributes to tissue damage. Thus, using these nanoparticles to deliver drugs that inhibit neutrophil recruitment to sites of chronic inflammation could limit such damage.[46] Antineutrophil recruitment drugs include reparixin and SB 225002 (*N*-(2-hydroxy-4-nitrophenyl)-*N*′-(2-bromophenyl)urea), which act on the neutrophil chemokine receptor (CXCR2) and inhibit neutrophil migration.[47,48] Cytotoxicity analysis of polymer **2** nanoparticles indicates that these are well-tolerated by both macrophages and stimulated neutrophils. In rheumatoid arthritis, polymer **2** nanoparticles could be injected directly into the joint cavity, while for COPD, nanoparticle administration would likely involve a nebulizer. Ongoing investigations are dedicated to investigating the potential of these polymeric systems to deliver therapeutic and diagnostic agents specifically to tissues undergoing oxidative stress.

ASSOCIATED CONTENT

Supporting Information

Experimental procedures for the synthesis of the polymer, characterization data (^{1}H NMR, ^{13}C NMR, ESI-MS), procedures for nanoparticles formulations, Nile Red and Paclitaxel release studies, effect of H_2O_2 on the fluorescence of Nile Red, additional SEM and TEM images, polymer degradation (GPC, ^{1}H NMR), cytotoxicity analysis of polymer **2** nanoparticles, calibration curves used for the Nile Red encapsulation efficiency determination. This material is available free of charge via the Internet at http://pubs.acs.org.

AUTHOR INFORMATION

Corresponding Author

aalmutairi@ucsd.edu

Notes

The authors declare no competing financial interest.

ACKNOWLEDGMENTS

We thank the NIH New Innovator Award (DP 2OD006499) and KACST for funding. We also thank Viet Anh Nguyen Huu for his help with experiments using nanoparticles encapsulating FDA.

REFERENCES

(1) Li, C. H.; Hu, J. M.; Liu, T.; Liu, S. Y. *Macromolecules* **2011**, *44*, 429.
(2) Van de Bittner, G. C.; Dubikovskaya, E. A.; Bertozzi, C. R.; Chang, C. J. *Proc. Natl. Acad. Sci. U.S.A.* **2010**, *107*, 21316.
(3) Sella, E.; Lubelski, A.; Klafter, J.; Shabat, D. *J. Am. Chem. Soc.* **2010**, *132*, 3945.
(4) Srikun, D.; Miller, E. W.; Dornaille, D. W.; Chang, C. J. *J. Am. Chem. Soc.* **2008**, *130*, 4596.
(5) Lee, D.; Khaja, S.; Velasquez-Castano, J. C.; Dasari, M.; Sun, C.; Petros, J.; Taylor, W. R.; Murthy, N. *Nat. Mater.* **2007**, *6*, 765.
(6) Chang, M. C. Y.; Pralle, A.; Isacoff, E. Y.; Chang, C. J. *J. Am. Chem. Soc.* **2004**, *126*, 15392.
(7) Yu, S. S.; Koblin, R. L.; Zachman, A. L.; Perrien, D. S.; Hofmeister, L. H.; Giorgio, T. D.; Sung, H. J. *Biomacromolecules* **2011**, *12*, 4357.
(8) Broaders, K. E.; Grandhe, S.; Frechet, J. M. J. *J. Am. Chem. Soc.* **2011**, *133*, 756.
(9) Wilson, D. S.; Dalmasso, G.; Wang, L. X.; Sitaraman, S. V.; Merlin, D.; Murthy, N. *Nat. Mater.* **2010**, *9*, 923.
(10) Rehor, A.; Hubbell, J. A.; Tirelli, N. *Langmuir* **2005**, *21*, 411.
(11) Napoli, A.; Valentini, M.; Tirelli, N.; Muller, M.; Hubbell, J. A. *Nat. Mater.* **2004**, *3*, 183.
(12) Khutoryanskiy, V. V.; Tirelli, N. *Pure Appl. Chem.* **2008**, *80*, 1703.
(13) Allen, B. L.; Johnson, J. D.; Walker, J. P. *ACS Nano* **2011**, *5*, 5263.
(14) Geronikaki, A. A.; Gavalas, A. M. *Comb. Chem. High Throughput Screening* **2006**, *9*, 425.
(15) Finkel, T. *Curr. Opin. Cell Biol.* **2003**, *15*, 247.
(16) Cachofeiro, V.; Goicochea, M.; de Vinuesa, S. G.; Oubina, P.; Lahera, V.; Luno, J. *Kidney Int.* **2008**, S4.
(17) Drechsel, D. A.; Patel, M. *Free Radic. Biol. Med.* **2008**, *44*, 1873.
(18) Liou, G. Y.; Storz, P. *Free Radical Res.* **2010**, *44*, 479.
(19) Esser-Kahn, A. P.; Odom, S. A.; Sottos, N. R.; White, S. R.; Moore, J. S. *Macromolecules* **2011**, *44*, 5539.
(20) Seo, W.; Phillips, S. T. *J. Am. Chem. Soc.* **2010**, *132*, 9234.
(21) Dewit, M. A.; Gillies, E. R. *J. Am. Chem. Soc.* **2009**, *131*, 18327.
(22) Murthy, N.; Xu, M. C.; Schuck, S.; Kunisawa, J.; Shastri, N.; Frechet, J. M. J. *Proc. Natl. Acad. Sci. U.S.A.* **2003**, *100*, 4995.
(23) Murthy, N.; Thng, Y. X.; Schuck, S.; Xu, M. C.; Frechet, J. M. J. *J. Am. Chem. Soc.* **2002**, *124*, 12398.
(24) Sankaranarayanan, J.; Mahmoud, E. A.; Kim, G.; Morachis, J. M.; Almutairi, A. *ACS Nano* **2010**, *4*, 5930.
(25) Goodwin, A. P.; Mynar, J. L.; Ma, Y. Z.; Fleming, G. R.; Frechet, J. M. J. *J. Am. Chem. Soc.* **2005**, *127*, 9952.
(26) Fomina, N.; McFearin, C.; Sermsakdi, M.; Edigin, O.; Almutairi, A. *J. Am. Chem. Soc.* **2010**, *132*, 9540.
(27) Avital-Shmilovici, M.; Shabat, D. *Bioorg. Med. Chem.* **2010**, *18*, 3643.
(28) Heffernan, M. J.; Murthy, N. *Bioconjugate Chem.* **2005**, *16*, 1340.
(29) Petros, R. A.; DeSimone, J. M. *Nat. Rev. Drug Discovery* **2010**, *9*, 615.
(30) Jourden, J. L. M.; Daniel, K. B.; Cohen, S. M. *Chem. Commun. (Cambridge, U. K.)* **2011**, *47*, 7968.
(31) Jourden, J. L. M.; Cohen, S. M. *Angew. Chem., Int. Ed.* **2010**, *49*, 6795.
(32) Kuivila, H. G. *J. Am. Chem. Soc.* **1954**, *76*, 870.
(33) Kuivila, H. G.; Armour, A. G. *J. Am. Chem. Soc.* **1957**, *79*, 5659.
(34) Brown, H. C. *Tetrahedron* **1961**, *12*, 117.
(35) Haba, K.; Popkov, M.; Shamis, M.; Lerner, R. A.; Barbas, C. F.; Shabat, D. *Angew. Chem., Int. Ed.* **2005**, *44*, 716.

(36) Lee, H. Y.; Jiang, X.; Lee, D. W. *Org. Lett.* **2009**, *11*, 2065.
(37) Sella, E.; Shabat, D. *J. Am. Chem. Soc.* **2009**, *131*, 9934.
(38) Hodge, P.; ODell, R.; Lee, M. S.; Ebdon, J. R. *Polymer* **1996**, *37*, 1267.
(39) Halliwell, B.; Clement, M. V.; Long, L. H. *FEBS Lett.* **2000**, *486*, 10.
(40) Winterbourn, C. C.; Garcia, R. C.; Segal, A. W. *Biochem. J.* **1985**, *228*, 583.
(41) Norman, J. *Anaesthesist* **1985**, *34*, 311.
(42) Noguera, A.; Batle, S.; Miralles, C.; Iglesias, J.; Busquets, X.; MacNee, W.; Agusti, A. G. *Thorax* **2001**, *56*, 432.
(43) Quint, J. K.; Wedzicha, J. A. *J. Allergy Clin. Immunol.* **2007**, *119*, 1065.
(44) Wright, H. L.; Moots, R. J.; Bucknall, R. C.; Edwards, S. W. *Rheumatology (Oxford)* **2010**, *49*, 1618.
(45) Chou, R. C.; Kim, N. D.; Sadik, C. D.; Seung, E.; Lan, Y.; Byrne, M. H.; Haribabu, B.; Iwakura, Y.; Luster, A. D. *Immunity* **2010**, *33*, 266.
(46) Gernez, Y.; Tirouvanziam, R.; Chanez, P. *Eur. Respir. J.* **2010**, *35*, 467.
(47) White, J. R.; Lee, J. M.; Young, P. R.; Hertzberg, R. P.; Jurewicz, A. J.; Chaikin, M. A.; Widdowson, K.; Foley, J. J.; Martin, L. D.; Griswold, D. E.; Sarau, H. M. *J. Biol. Chem.* **1998**, *273*, 10095.
(48) Zarbock, A.; Allegretti, M.; Ley, K. *Br. J. Pharmacol.* **2008**, *155*, 357.